Solar Cycle Properties From Schwabe Data

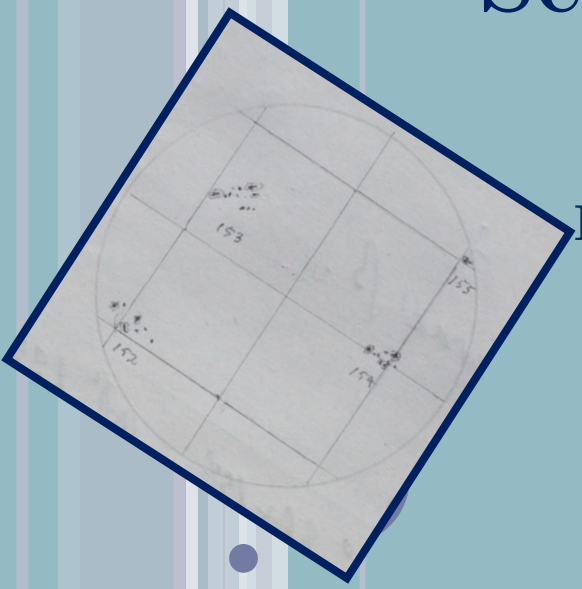

V. Senthamizh Pavai , Rainer Arlt

Leibniz Institute for Astrophysics Potsdam

Overview:

- Introduction
- Sunspot drawings by Samuel Heinrich Schwabe during 1825 - 1867
- Estimation of true umbral area values for 12 different sized cursors.
- Regrouping of sunspot groups
- Tilt angle calculation
- Testing the empirical relations used in reconstruction of solar butterfly diagram:
- Surface Flux Transport Model
- Conclusion

Introduction:

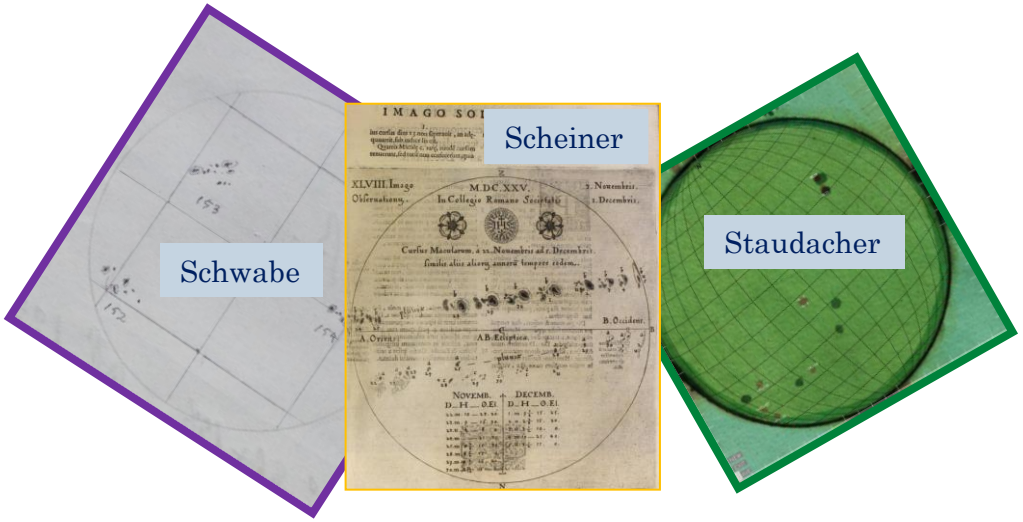

Significance of historical sunspot observations:

Better understanding of solar cycle

Long term global properties of solar magnetic field

- provides important constraints for models of the Sun's global dynamo
- relevant for studies of the past terrestrial climate

Evolution of radial magnetic field before 20th century can be inferred from the distribution of sunspots.

With latitude, longitude and area of sunspots; total and open flux can be reconstructed .

Total surface flux – integrated unsigned magnetic field over the whole surface.

Open flux – unsigned radial component of the magnetic field at the orbit of Earth.

Sunspot drawings by Samuel Heinrich Schwabe:

Location: Dessau, Germany.

Sunspot observations: Oct 1, 1825 – Dec 31, 1867, solar cycle 7 – 10 .

8500 full-disk drawings of the Sun and verbal notes.

Drawn with pencil in a circle of 5 cm diameter.

Observing books (39) are stored in Royal Astronomical Society, London.

1825 – 1830: disk drawings and magnification of the groups.
1831 – 1867: only disk drawings at higher detail.

Observations have been digitized. Positions and sizes of sunspots were measured by Arlt et al. (2013).

Sizes of the sunspots were determined using 12 different circular-shaped cursors.

The problem is that the sunspot areas are not drawn to-scale and require a conversion to true areas in km^2 or millionths of a solar hemisphere (MSH).

Two styles of Schwabe's sunspot drawings:

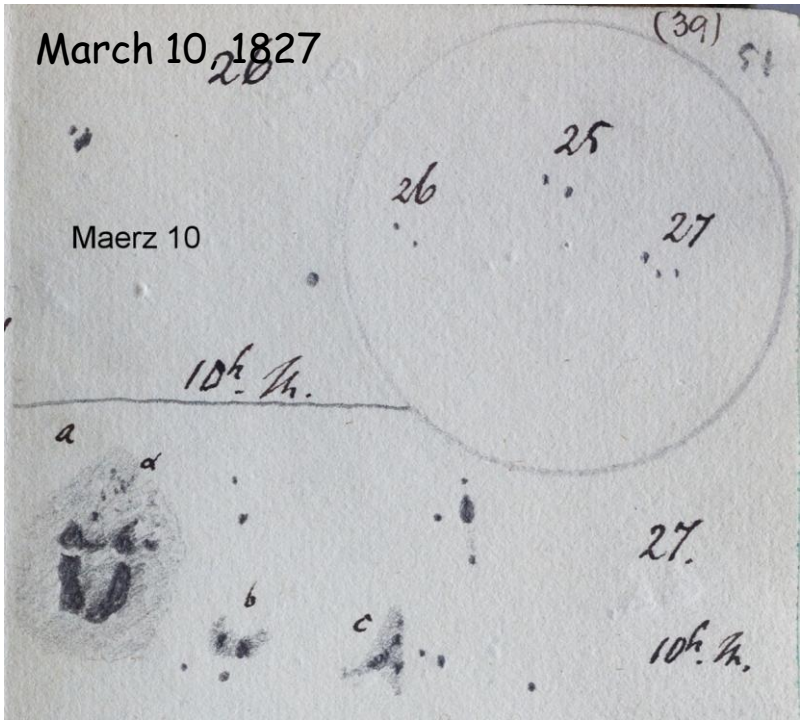

1825 – 1830:

Spots include umbra and penumbra

Data source used in area estimation:
Debrecen

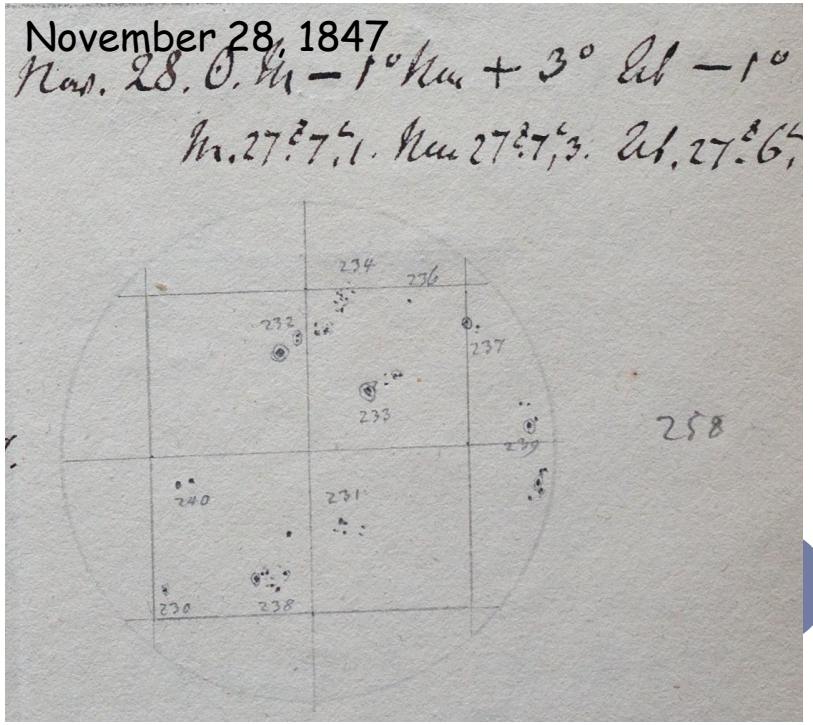

1831 – 1867:

Umbra and penumbra are distinguished

Data sources used:
Debrecen, MDI, Kodaikanal, Mt. Wilson

Estimation of true umbral area values for 12 different sized cursors:

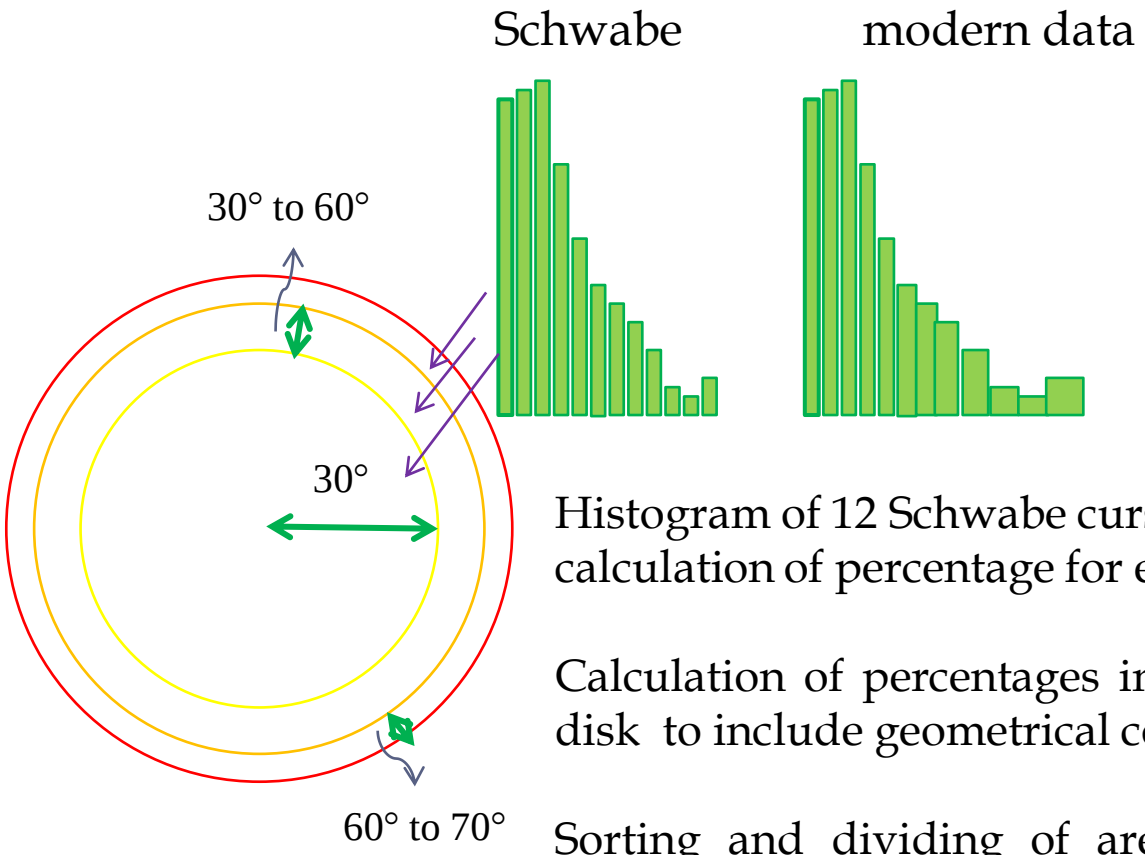

Histogram of 12 Schwabe cursor sizes/classes → calculation of percentage for each class.

Calculation of percentages in three different regions of disk to include geometrical correction.

Sorting and dividing of area values of various data sources based on the percentage of Schwabe size classes for various regions of the disk.

Average area values of each classes in 3 regions of the disk.

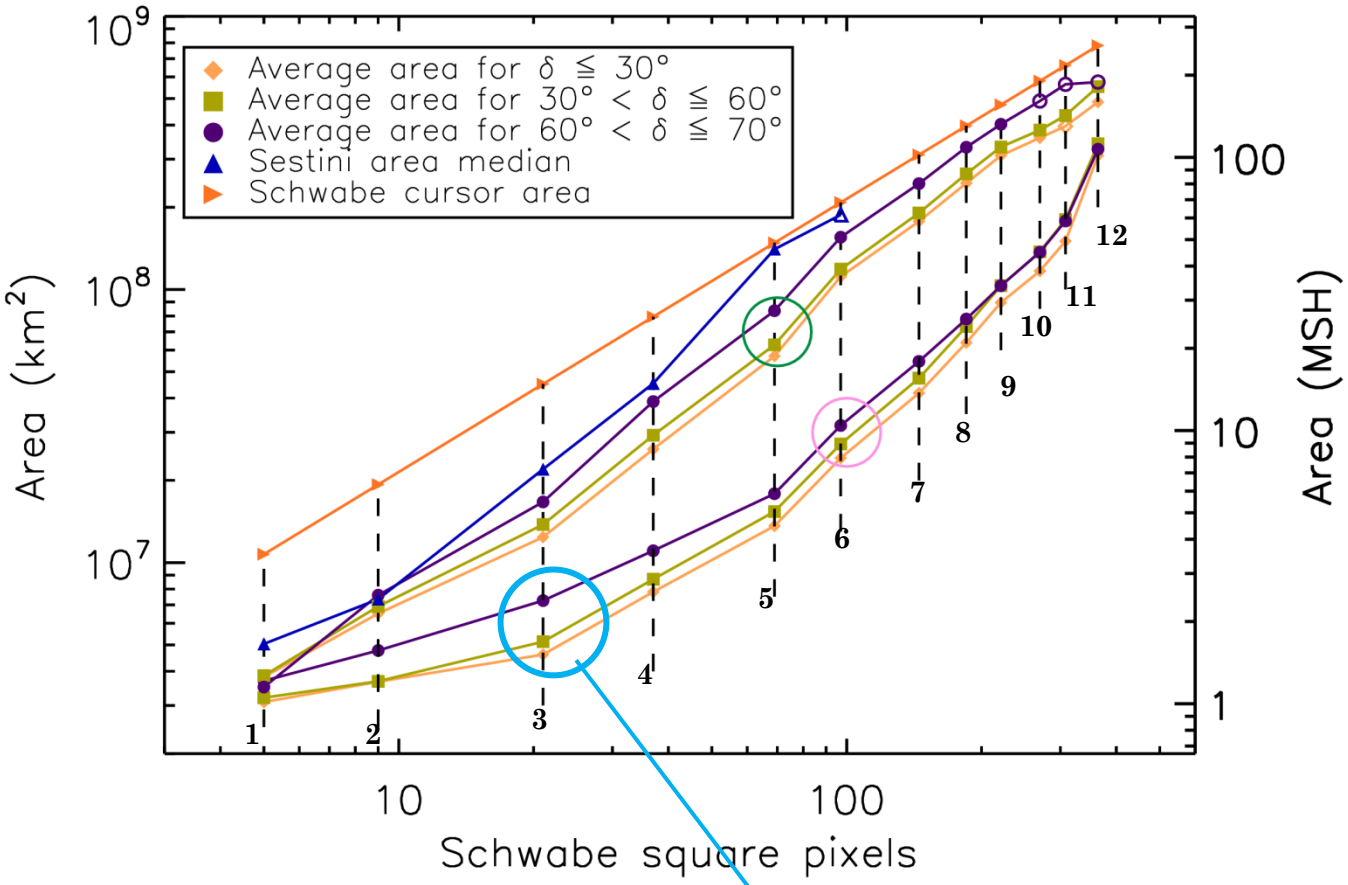

Average area during
a 1831 – 1867
b 1826 – 1830

$$Area = \frac{A_i}{\cos\delta} + B_i$$

δ - distance from disk centre

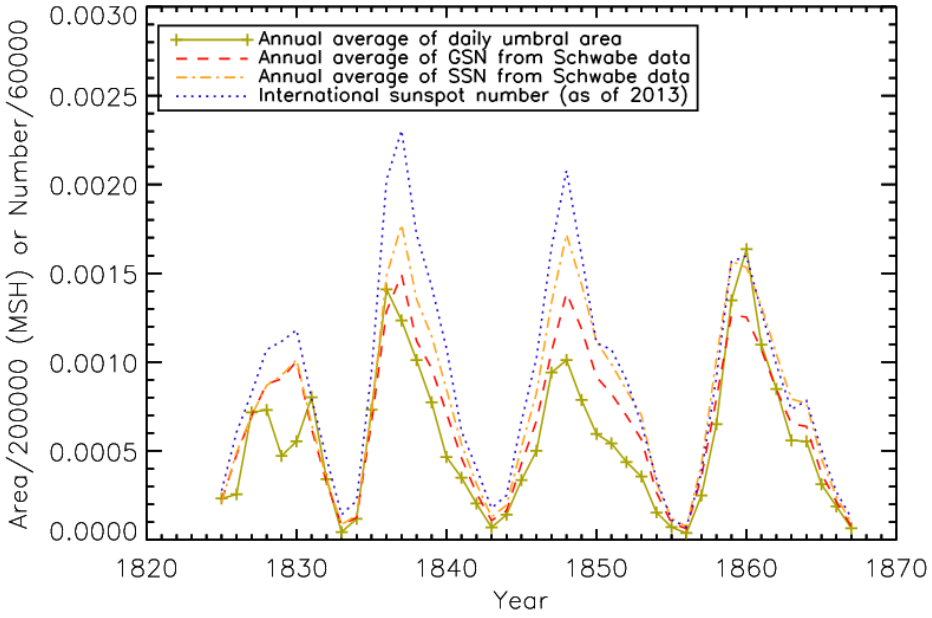

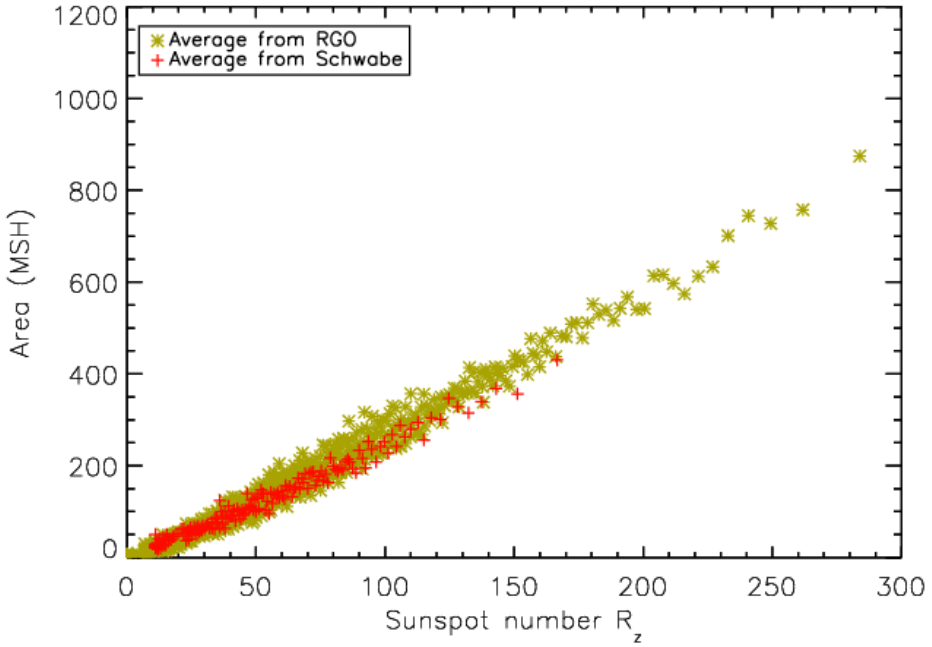

Area values show different trend compared to sunspot numbers.

Area range lies within the Greenwich sunspot area.

Area distribution:

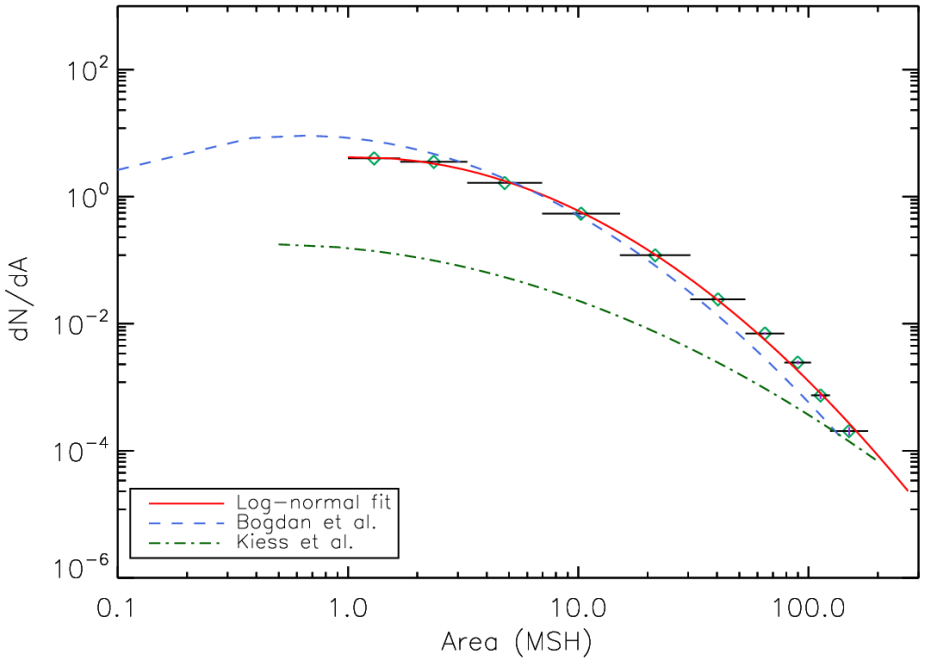

134 390 spots in Schwabe data

133 500 spots with position

For distribution studies:

Spots within ±50° CMD and ±45° latitude

$$\frac{dN}{dA} = \frac{\Delta N}{\Delta A} \frac{(180°/100°)}{N_{observeddays}}$$

On log-log plot, size distribution appears to be parabolic – lognormal distribution

$$\ln\left(\frac{dN}{dA}\right) = -\frac{(\ln A - \ln\langle A\rangle)^2}{2\ln\sigma_A} + \ln\left(\frac{dN}{dA}\right)_{\max}$$

dN/dA – Gaussian distributions in ln A

$\langle A\rangle$, σ_A – mean and geometric standard deviation

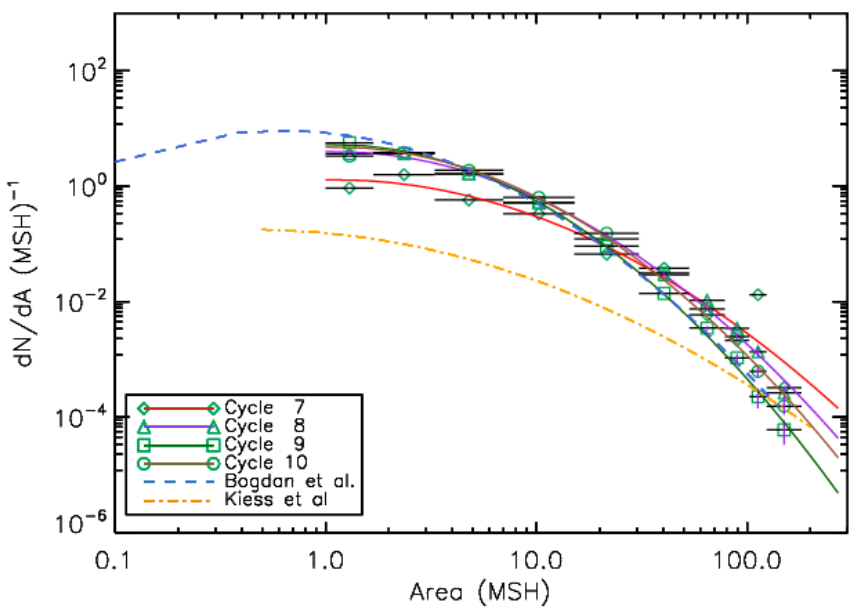

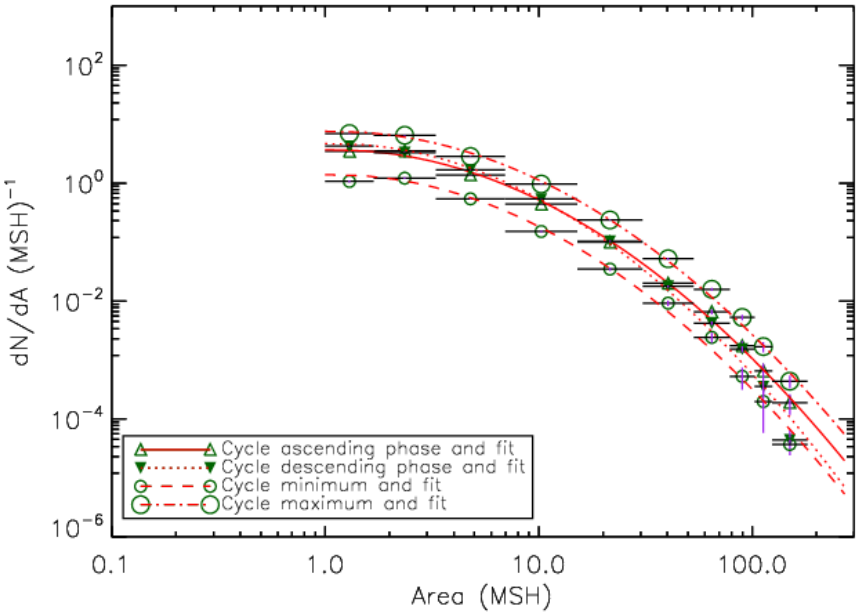

Distribution of area values are independent of time. Similar to Bogdan et al. (1998) distribution curves.

Data	N spots	‹A›	σ_A	$(dN/dA)_{max}$
All data (1825 - 1867)	104216	1.05	3.80	3.8
1831 – 1867	96983	1.10	3.49	4.2
1825 – 1830	7233	0.58	9.90	1.7
Cycle 7	9448	1.09	5.3	1.3
Cycle 8	22381	1.08	3.80	4.0
Cycle 9	36862	1.08	2.99	5.3
Cycle 10	35181	1.10	3.39	4.9
Ascending phases	13613	1.09	3.49	3.7
Descening phases	46763	1.10	3.09	4.7
Cycle minima	3507	1.08	3.39	1.4
Cycle maxima	31130	1.10	3.59	7.6

Regrouping of sunspot groups:

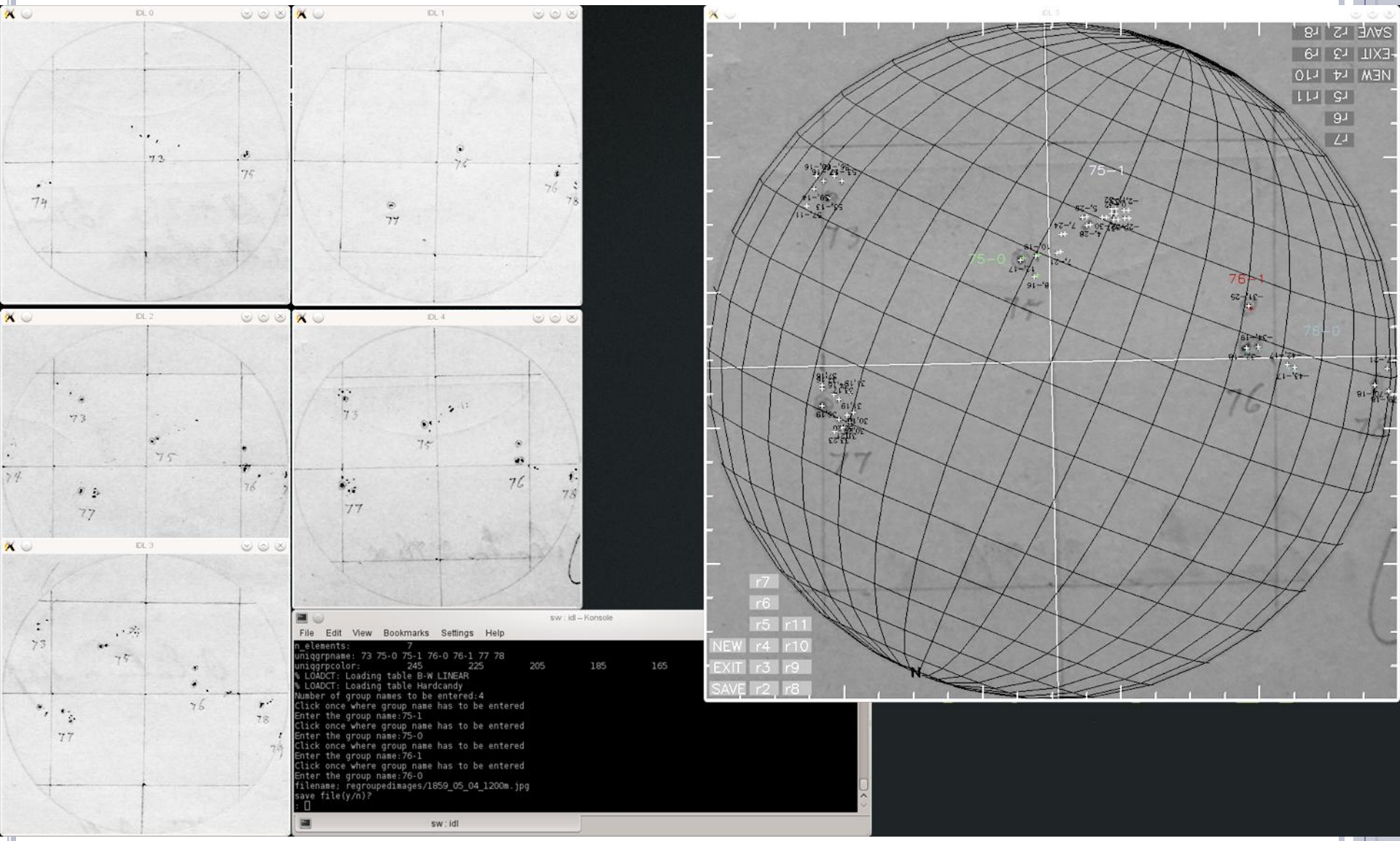

Group sunspot number, R_G

$$R_G = \frac{12.08}{n} \sum_{i=1}^{n} k_i G_i$$

G_i- number of sunspot groups

k_i – correction factors for observers (n)

R_G after regrouping and Hoyt & Schatten's are similar.

Average number of spots in a group from magnifications are close to modern value - good.

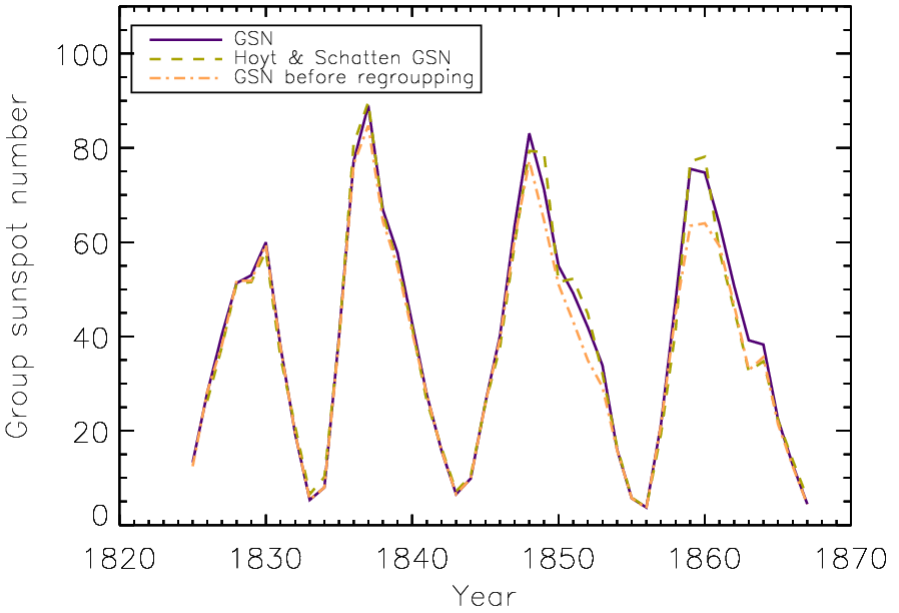

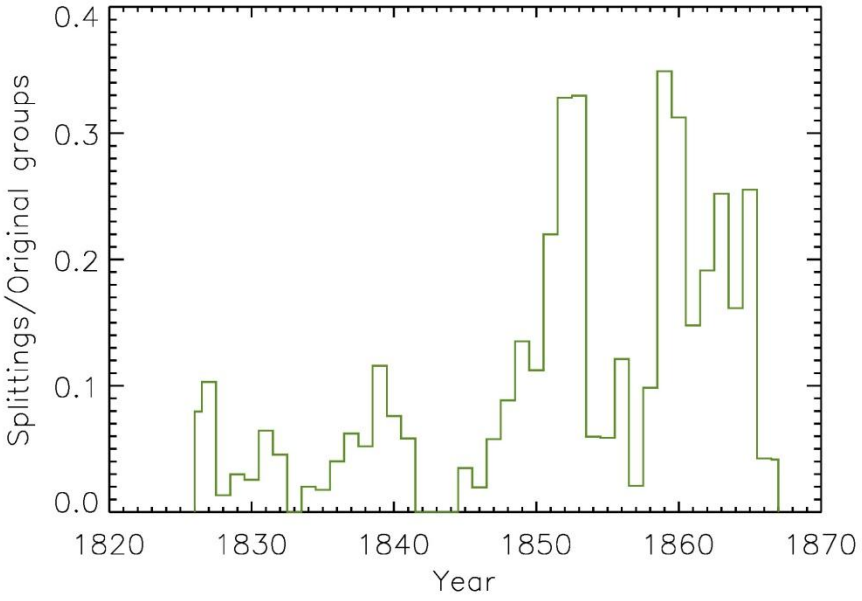

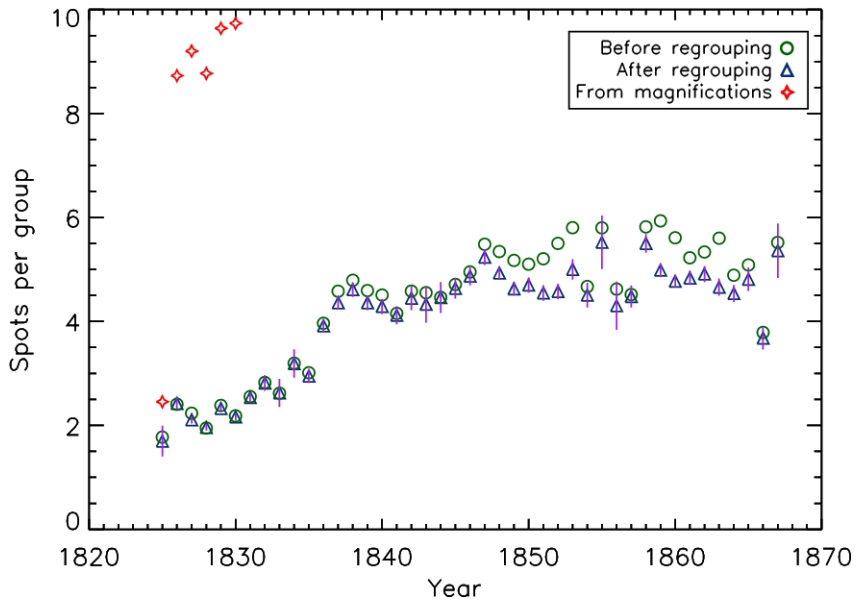

Tilt angle calculation:

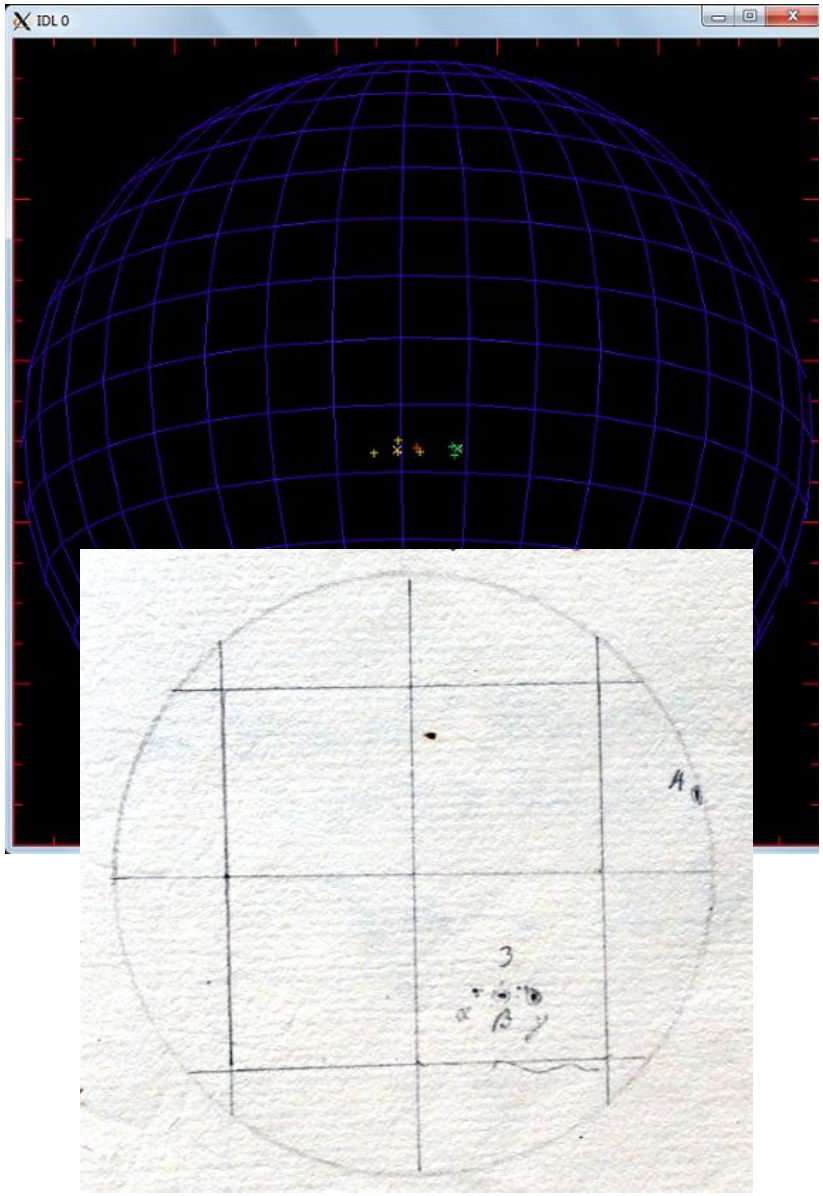

Groups are divided into two polarities with the lowest variance with which it can be divided.

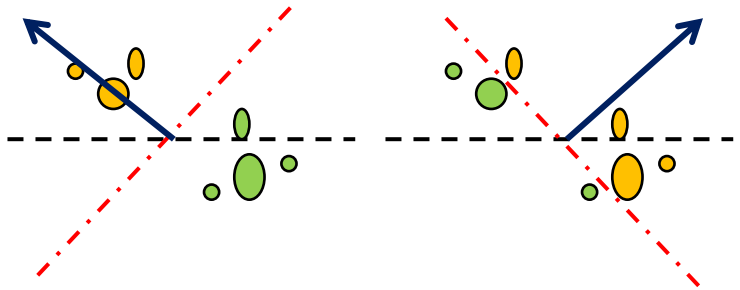

Tilt angles are calculated in its tangential plane:

$$\theta = \arctan\left(\frac{\Delta P_x}{\Delta P_y}\right)$$

varies from 90° to -90°
pseudo-tilt angle
no magnetic polarity information
reversed polarity cannot be found
The sign of tilt angle is positive if the leading part is closer to the equator.

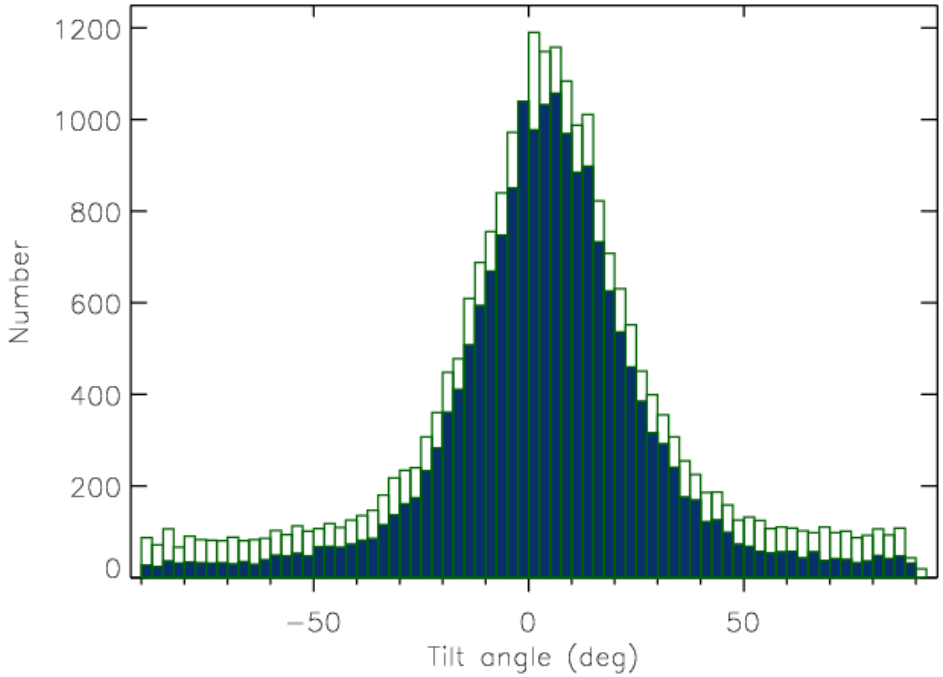

Histogram of the tilt angles of all groups (open). The filled histogram shows the distribution of tilt angles of groups with polarity separation > 3°.

For groups with polarity separation > 3°: Average tilt angle is 4.34 ± 0.19 deg.

Average tilt angle of Mt. wilson sunspot groups is 4.2 ± 0.2 deg

Tilt angles can affect polar field and open magnetic flux

(Howard, R. F. 1991, *Sol. Phys.*, 136, 251)

Schwabe: 1825 - 1867

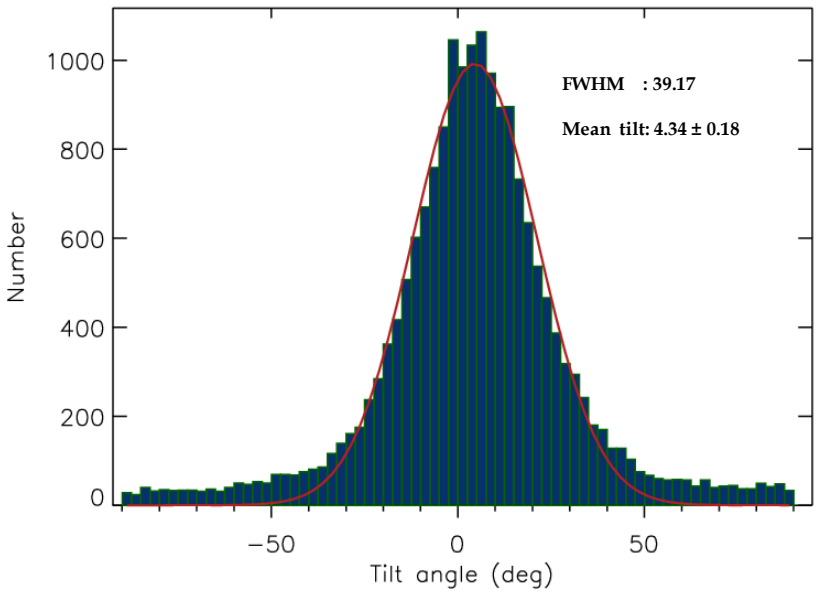

Scheiner drawings – 18 years before Maunder minimum. But the mean tilt angle does not seem to differ.

Decrease in mean tilt angle for Staudacher observations are due to the less precise drawings.

Scheiner: 1618, 1621, 1622, 1624, 1625-1627

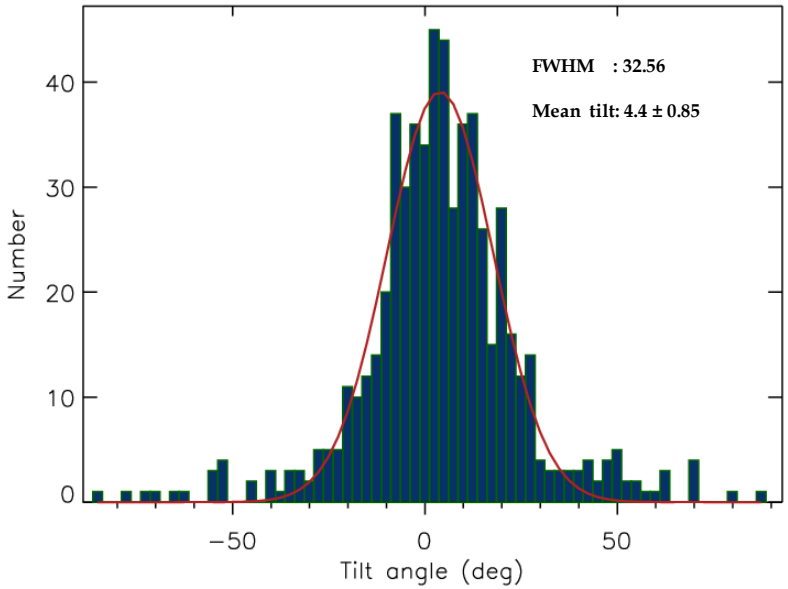

Staudacher: 1749 - 1796

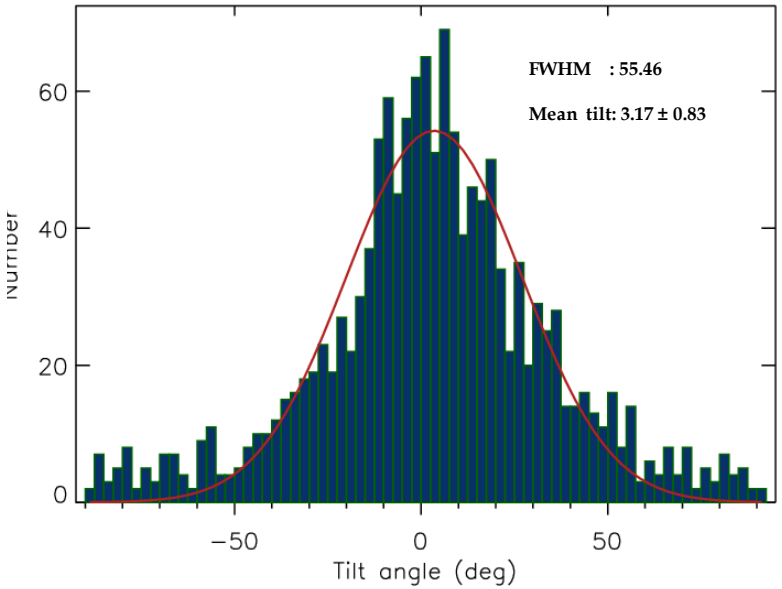

Testing the empirical relations in reconstruction of solar butterfly diagram:

Synoptic record of sunspot emergence is an important input for

- long term reconstructions of the solar open flux
- solar irradiance variations
- understanding solar dynamo, Babcock - Leighton type dynamos in particular.

Parameters needed

- Sunspot areas
- Emergence latitudes and longitudes
- Tilt angle

Record of sunspot emergence is not completely available before 1826 but sunspot numbers are available back to 1610.

- Monthly Wolf sunspot number from 1749
- Yearly Wolf sunspot number from 1700 – 1748
- Monthly group sunspot from 1610

Jie et al. 2011 have derived empirical relations for reconstruction of sunspot group emergence. Greenwich sunspot group data (1874 - 1976) has been used to derive the relation between solar cycle strength and reconstruction parameters.

Latitude distribution:

Mean latitude of emergence during cycle n is

$\lambda_n = 12.2 + 0.022\, S_n$

S_n - maximum of the 12 month running mean of R_G of cycle n.

Phase (i) dependence of mean latitude of emergence for cycle n

$$\lambda_n^i = (26.4 - 34.2(i/30) + 16.1(i/30)^2)(\lambda_n / \langle \lambda_n \rangle_{12\text{-}20})$$

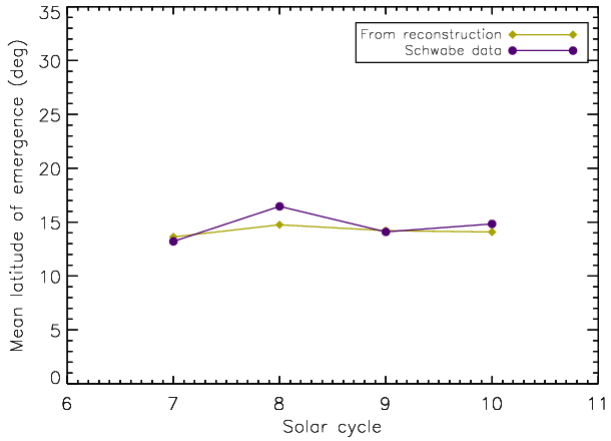

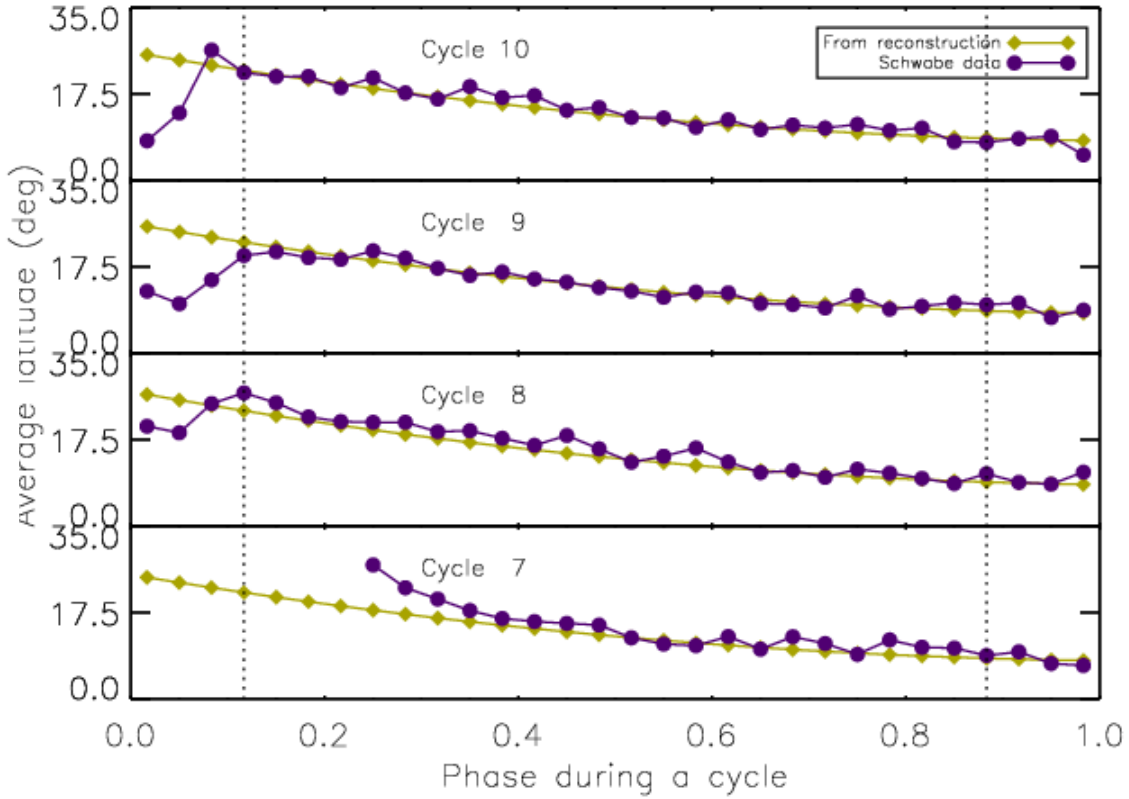

Tilt angle distribution:

Average tilt angle,

$$\alpha_n = T_n \sqrt{|\lambda|}$$

T_n – constant for a cycle which is given by

$$T_n = 1.73 - 0.0035 S_n$$

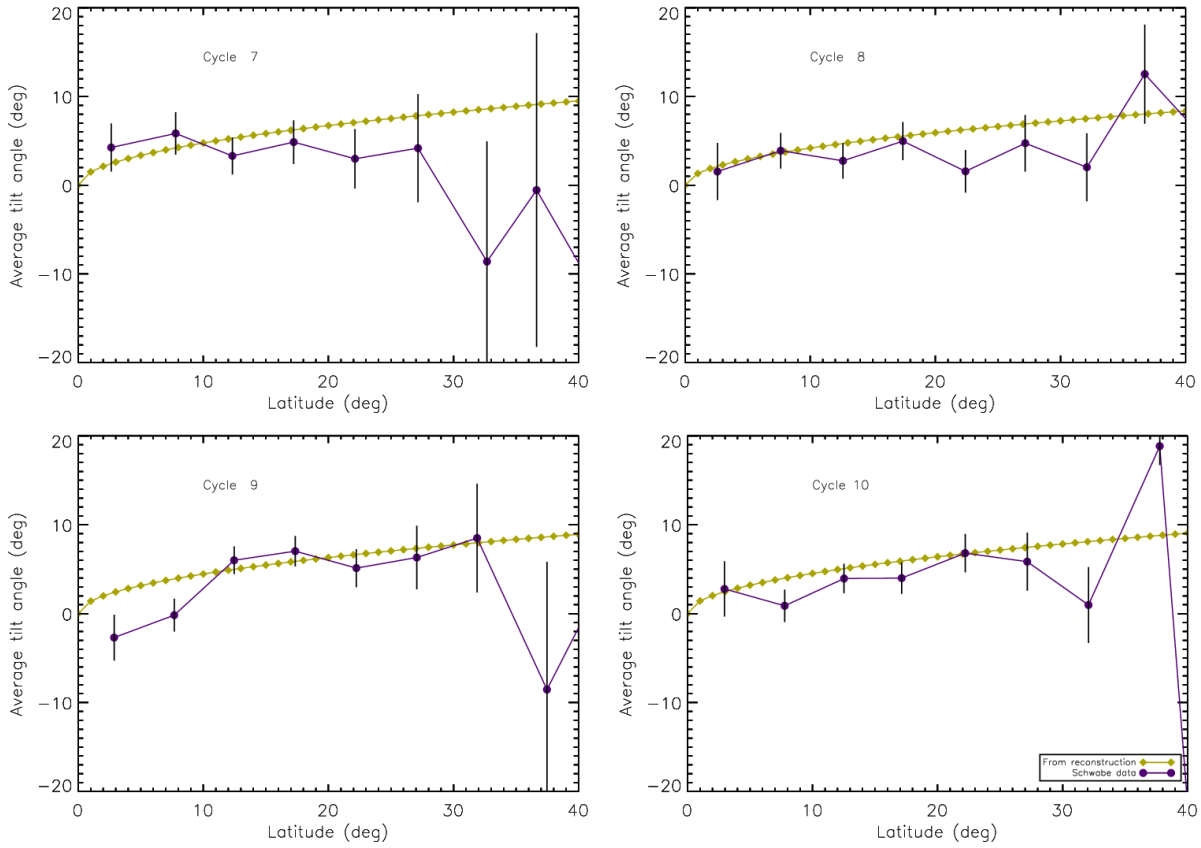

Surface Flux Transport Model (SFTM):

SFTM uses the distributions of emerging active regions to inject radial magnetic field. Then the evolution of this flux under the influence of meridional flows, differential rotation and turbulent magnetic diffusivity is simulated.

The equation governing the SFTM is:

$$\frac{\partial B_r}{\partial t} = -\Omega(\theta)\frac{\partial B_r}{\partial \phi} - \frac{1}{R_\odot \sin\theta}\frac{\partial}{\partial \theta}\left[v(\theta)B_r \sin\theta\right] + \frac{\eta_h}{R_\odot^2}\left[\frac{1}{\sin\theta}\frac{\partial}{\partial\theta}\left(\sin\theta\frac{\partial B_r}{\partial\theta}\right) + \frac{1}{\sin^2\theta}\frac{\partial^2 B_r}{\partial\phi^2}\right]$$

$$-D_r(\eta_r) + S(\theta,\phi,t)$$

$S(\theta,\phi,t)$ – source term – emergence of new magnetic flux

$D_r(\eta_r)$ – decay term – radial loss of magnetic flux

$\Omega(\theta)$ – differential rotation

$v(\theta)$ – meridional flow

η_h - turbulent surface diffusivity

η_r – radial diffusivity

input from above-mentioned relations

source term:
latitudes & longitudes of polarities of active region and angular separation of polarities during group maximum.

Active region area (A_R) from sunspot area:

Total sunspot area, $A_s = 5 * A_u$ (Brandt et al. 1990)

$A_R = A_s + A_p = A_s + 414 + 21A_s - 0.0036A_s^2$ (Chapman et al. 1997)

The locations of the bipolar magnetic regions can be derived from the locations of sunspot groups. (Cameron et al. 2010)
In northern hemisphere,

$$\lambda_{\pm} = \lambda_m \pm (-1)^n 0.5\Delta\beta \sin\alpha, \quad \phi_{\pm} = \phi_m \mp (-1)^n 0.5\Delta\beta \cos\alpha (\cos\lambda_m)^{-1}$$

In southern hemisphere,

$$\lambda_{\pm} = \lambda_m \pm (-1)^n 0.5\Delta\beta \sin\alpha, \quad \phi_{\pm} = \phi_m \pm (-1)^n 0.5\Delta\beta \cos\alpha (\cos\lambda_m)^{-1}$$

$$\Delta\beta = 0.45A_R^{1/2} \qquad \alpha_n = T_n\sqrt{|\lambda|}$$ (from Kodaikanal and Mt. Wilson data)

$\lambda_{\pm}$, $\phi_{\pm}$ - latitudes and longitudes of polarities respectively
$\Delta\beta$ – polarity separation

Magnetic butterfly diagram:

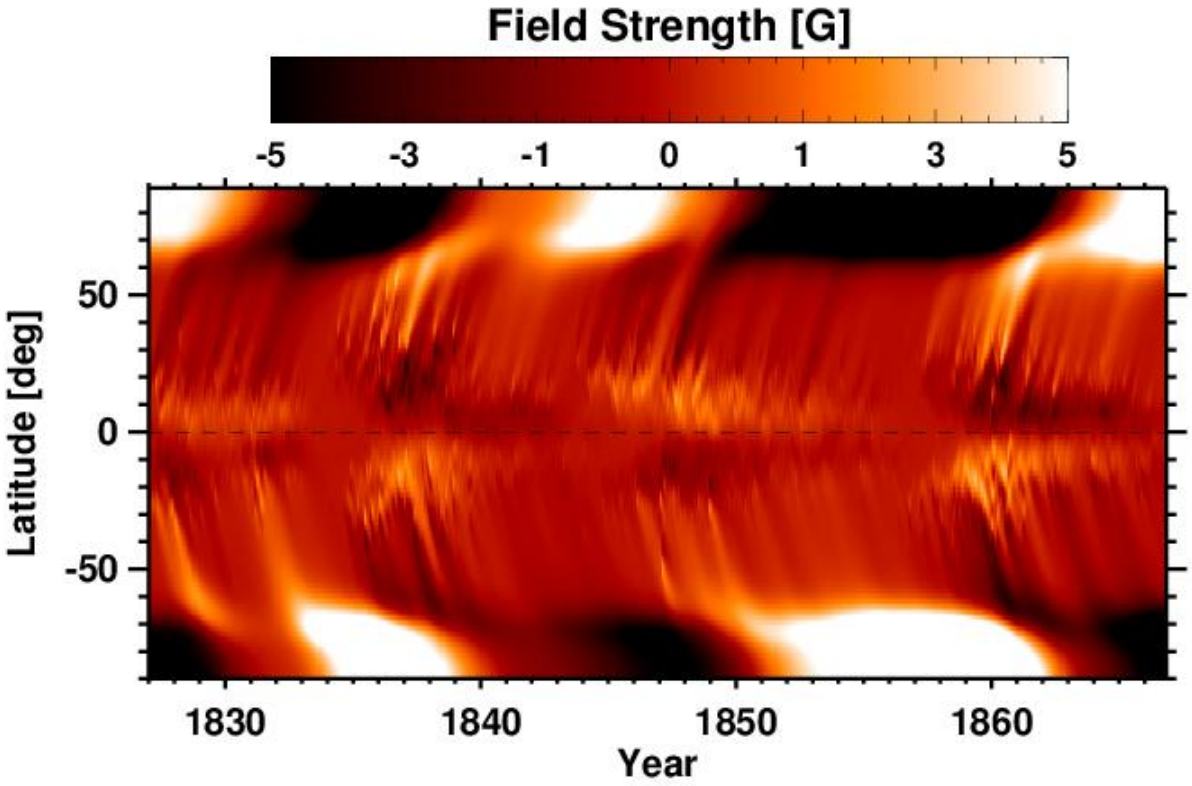

$\eta_H = 2.5 \times 10^{12}$ cm^2 s^{-1}
$\eta_r = 0$
$B_0 = -10.2$ G
$R_{cusp} = 1.55$ solar radius

The heliospheric open flux can be extrapolated from the distribution of surface flux using the Current Sheet Source Surface (CSSS) Model.

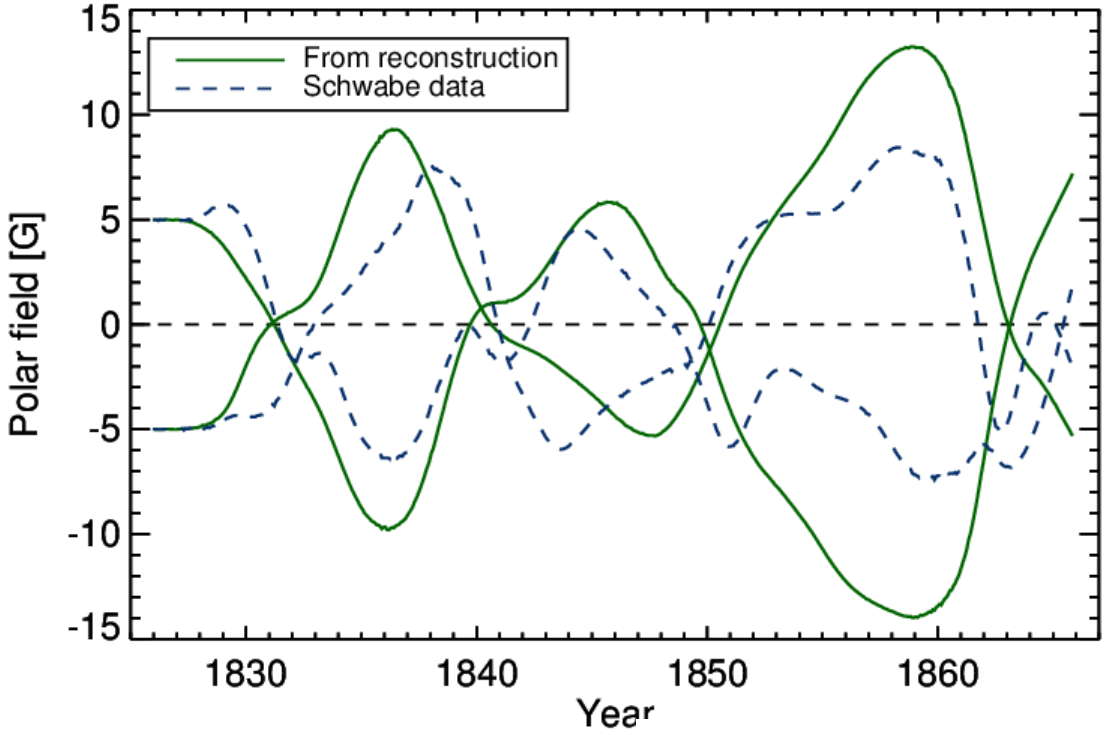

From SFTM:

27 day averaged north and south polar field

Polar field – average over a polar cap of 15° latitude

Maximum of the unsigned north-south averaged polar fields correlated with the amplitude of the next cycle.

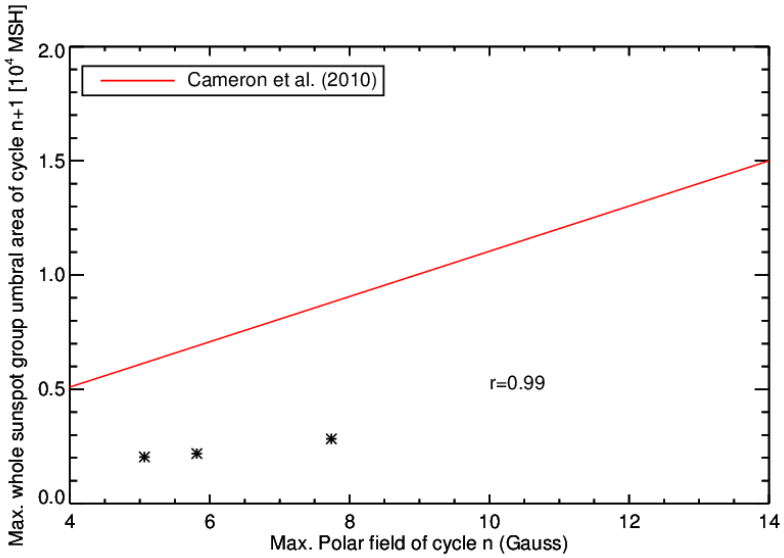

Conclusion:

The sunspot positions, areas and tilt angles are now available for the solar cycle 7 – 10.

Surface magnetic field has been derived using Surface Flux Transport model.

The method of reconstruction of sunspot emergence using sunspot numbers were tested for Schwabe data and seems to work. It can be upgraded using Schwabe data together with Greenwich data.

Mean tilt angle does not seem to vary before and after the Maunder minimum.

References:

Thank You

Differential rotation profile – Snodgrass (1983)

$$\Omega(\lambda) = 13.38 - 2.30\sin^2\lambda - 1.62\sin^4\lambda$$

Meridional flow – van Ballegooijen et al. (1998)

$$v(\lambda) = \begin{cases} 11\sin(2.4\lambda) ms^{-1} & \text{where } |\lambda| \le 75° \\ 0 & \text{otherwise} \end{cases}$$

The initial distribution of the radial field of a new bipole,

$$B = B^+ - B^-$$

$$B^{\pm}(\lambda,\phi) = B_{\max}\left(\frac{0.4\Delta\beta}{\delta}\right)^2 \exp\left(2\left[1-\cos\left(\beta_{\pm}(\lambda,\phi)\right)/\delta^2\right]\right)$$

B+, B- are the distributions of the positive and negative polarity flux at the solar surface.
$0.4\Delta\beta$ – initial angular width of each component,
$\delta = 4°$ is the size of the individual polarity patches.

Active regions inserted into model at $\delta = 4°$.

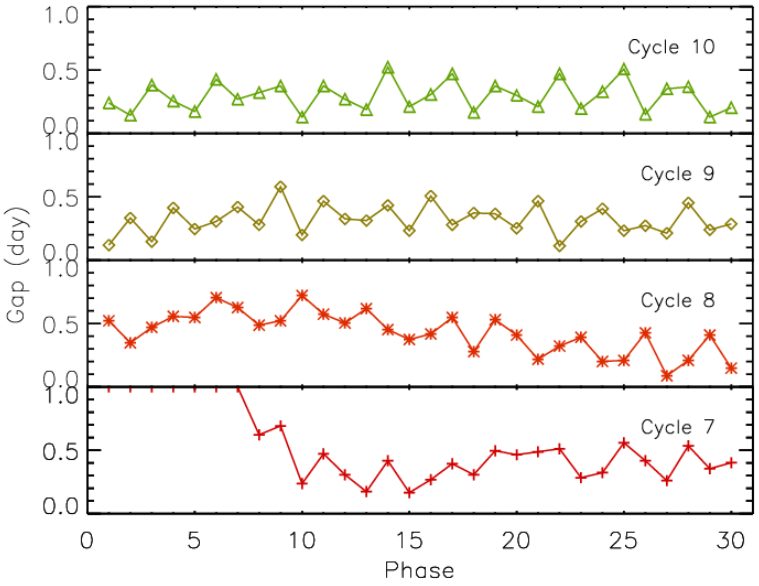
Cycle 10
Cycle 9
Cycle 8
Cycle 7
Gap (day)
Phase

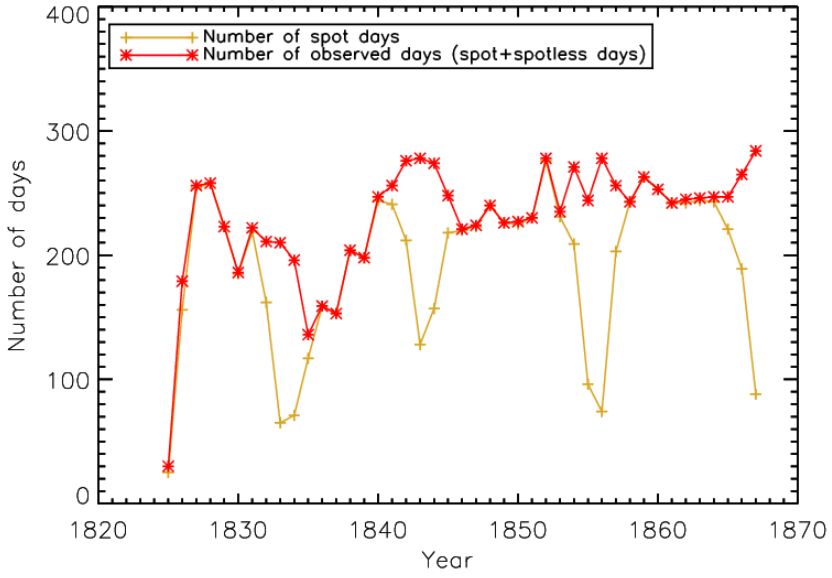
Number of spot days
Number of observed days (spot+spotless days)
Number of days
Year

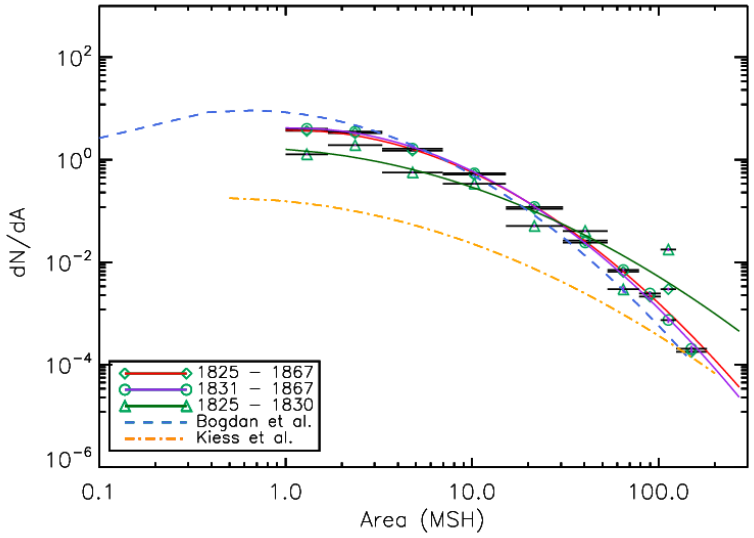
1825 – 1867
1831 – 1867
1825 – 1830
Bogdan et al.
Kiess et al.
dN/dA
Area (MSH)

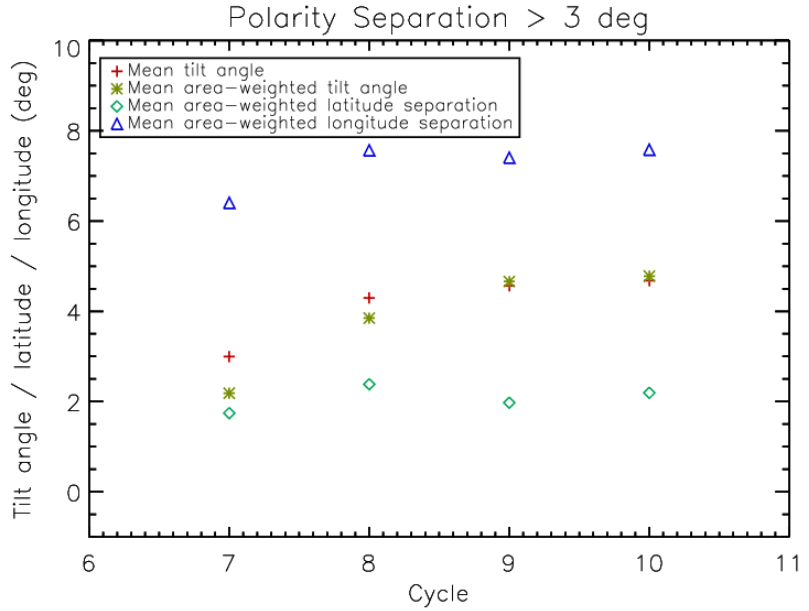
Polarity Separation > 3 deg
Mean tilt angle
Mean area–weighted tilt angle
Mean area–weighted latitude separation
Mean area–weighted longitude separation
Tilt angle / latitude / longitude (deg)
Cycle